Cellular Physiology and Biochemistry
Cell Physiol Biochem 2015;36:2217-2228
DOI: 10.1159/000430186
Published online: July 24, 2015
Accepted: May 04, 2015

1421-9778/15/0366-2217$39.50/0

Original Paper

PRDX6 Protects ARPE-19 Cells from Oxidative Damage via PI3K/AKT Signaling

Xu Zha Guojiu Wu Xueying Zhao Liqiong Zhou Hong Zhang Jinghua Li Linkun Ma Yuanping Zhang

Department of the Ophthalmology, the Second Affiliated Hospital of Kunming Medical University, Kunming, China

Key Words
ARPE-19 • PRDX6 • Oxidative stress • Apoptosis • PI3K/AKT signaling pathway

Abstract
Background/Aims: Oxidative stress that damages cells of the retinal pigment epithelium (RPE) can cause the development of hereditary retinal disease (HRD). PRDX6, which is a member of the PRDX family, is essential for removing metabolic free radicals from the body. However, the effect of PRDX6 on oxidative stress in HRD remains unknown. In this study, we sought to investigate the role of PRDX6 in oxidative stress-induced HRD in ARPE-19 cells and the molecular mechanism involved. ***Methods:*** ARPE-19 cells were used in the current study. Intracellular ROS levels were determined by flow cytometry. Lipid peroxidation was measured using a commercial MDA assay kit. Cellular variability was determined by MTT assay. Apoptosis was determined using an Annexin V-FITC Apoptosis Detection Kit. mRNA and protein expression levels were detected by real-time PCR and western blot analysis, respectively. ***Results:*** We found that H_2O_2 and blue light could induce significant oxidative stress damage and cell death in ARPE-19 cells. Furthermore, we found that PRDX6 levels significantly decreased after H_2O_2 treatment. PRDX6 overexpression protected ARPE-19 cells from H_2O_2- and blue light-induced oxidative damage, while PRDX6 knockdown enhanced oxidative damage in these cells. Mechanistically, we found that PRDX6 prevented oxidative damage and promoted ARPE-19 cell survival through the PI3K/AKT signaling pathway. ***Conclusions:*** Collectively, these results suggest that PRDX6 protects ARPE-19 cells from H_2O_2-induced oxidative stress and apoptosis and that this protection is mediated at least partially through the PI3K/AKT pathway.

Yuanping Zhang

Department of the Ophthalmology, The second Affiliated Hospital of Kunming Medical university, Kunming, China, 650101 (China)
Tel. +86-0871-65137443, Fax +86-0871-65137443, E-Mail zhangyuanpingbio@163.com

Introduction

Hereditary retinal disease (HRD) is primary retinal degeneration that can lead to severe visual impairments and refractory blindness [1]. The average incidence of HRD is approximately 1/3000 in developed countries, although its average incidence in China is much higher (1/1000) [2, 3]. Among blindness-causing eye diseases, HRD has the highest incidence in the global working-age population. Therefore, HRD has received international attention in ophthalmology.

The retinal pigment epithelium (RPE), which is in the outermost layer of the retina, plays an extremely important physiological role in maintaining photoreceptor function and structure [4]. Unfortunately, RPE cells are susceptible to oxidative stress induced by their own metabolic products. Growing evidence has shown that oxidative damage causes HRD [5, 6]. *In vitro*, oxidative stress has been reported to cause damage to RPE cells, leading to photoreceptor cell apoptosis, which subsequently contributes to the pathogenesis of HRD [2, 7]. *In vivo*, HRD mice were found to be more vulnerable to short-wavelength radiation due to higher reactive oxygen species (ROS) production compared to WT mice [8].

Peroxiredoxin 6 (PRDX6) is a protein found in mammals [9-12] that belongs to PRDX, a newly identified antioxidant family. PRDX6 was first isolated from bovine ciliary proteins by Shichi et al. and named non-selenium-dependent glutathione peroxidase [13]. Functionally, PRDX6 removes metabolically produced free radicals in the body by neutralizing peroxides, peroxynitrite, and phospholipid hydroperoxides [14]. PRDX6 is involved in many different diseases, such as diabetes, cancer, and lung damage [15, 16]. Additionally, PRDX6 plays a role in oxidative damage in a lung epithelial cell line. For instance, PRDX6 overexpression significantly decreased oxidative stress-induced lipid peroxidation and cell membrane damage [15]. In contrast, RNA silencing of PRDX6 in rat lung epithelial cells markedly increased lipid peroxidation, cell membrane damage and apoptosis upon oxidative stress stimulation [17]. However, whether PRDX6 plays a role in oxidative damage to the RPE and whether its dysfunction contributes to HRD progression remain undetermined.

In the present study, we used H_2O_2 and blue light to induce oxidative damage in ARPE-19 cells and demonstrated for the first time a protective role for PRDX6 against oxidative damage in ARPE-19 cells. Mechanistically, we found that PRDX6 protected cells from oxidative damage through the PI3K/AKT pathway. These findings not only defined the role of PRDX6 in oxidative damage to the RPE but also provided a potential therapeutic target for future HRD treatment.

Material and Methods

Reagents

The human RPE cell line ARPE-19 was obtained from American Type Culture Collection (ATCC, USA). Assay kits for MTT, MDA and ROS were purchased from Beyotime (Nantong, China). The antibodies for p-AKT, AKT and β-actin were obtained from Santa Cruz Biotechnology (Santa Cruz, CA). The PI3K/AKT signaling pathway inhibitor LY294002 was purchased from Selleck Company. Dulbecco's modified Eagle's medium and fetal bovine serum were obtained from Gibco BRL (Grand Island, NY). An annexin V-fluorescein isothiocyanate (FITC)-propidium iodide (PI) apoptosis kit was purchased from Becton Dickinson (Mountain View, CA).

Cell culture

ARPE-19 cells were cultured in Dulbecco's modified Eagle's medium supplemented with 10% (v/v) heat-inactivated fetal bovine serum, 100 μg/ml streptomycin, and 100 U/ml penicillin. The cells were incubated at 37°C in a humidified 5% CO_2 atmosphere, and the medium was changed every other day. The cells were grown to an appropriate density and used at passages 10–15.

MTT assay

Cell viability was measured by quantitative colorimetric MTT assay (Beyotime, Nantong, China). Briefly, ARPE-19 cells were seeded in 96-well plates (6×10^3 cells/well) and maintained in growth media for 24 h with 5% CO_2 at 37°C. When the cells reached 60% confluence, they were treated with 0–1 mmol/l H_2O_2 and blue light (470 ±20 nm) for 24 h. Next, 10 µl of MTT solution (5 mg/ml) was added to each well, and the cells were incubated for another 4 h at 37°C. After formazan crystals formed, the MTT medium was aspirated and replaced with 150 µl of dimethyl sulfoxide (DMSO) (Beyotime, Nantong, China) to solubilize the crystals. Then, the plates were shaken for 5 min. The absorbance of each well was recorded using a microplate spectrophotometer at 570 nm. Relative cellular growth was determined by the ratio of the average absorbance of treated cells versus the average absorbance of control cells. Cell viability was calculated as the ratio of optical densities.

Detection of intracellular ROS levels

To measure ROS generation within H_2O_2-treated cells, FACS analysis was performed. Briefly, cells were exposed to H_2O_2 for the indicated times and then stained with 5 µg/ml DCF-DA (Beyotime, Nantong, China) for 30 min. Next, the cells were subjected to flow cytometry using a Partec CyFlow flow cytometer (Partec, Germany) and analyzed using FloMax 2.82 software.

Determination of cellular lipid peroxidation via MDA assay

Malondialdehyde (MDA), an end product of lipid peroxidation, was measured to estimate the levels of lipid peroxidation in ARPE-19 cells using a commercial MDA assay kit (Beyotime). The results are expressed as nM/mg protein.

8-Hydroxy-2'-deoxyguanosine (8-OHdG) ELISA

The 8-OHdG content in lysis solution was detected by ELISA. A human 8-OHdG ELISA kit was purchased from Cusabio Biotech Company (Wuhan, China) and used according to the manufacturer's instructions.

Analysis of apoptosis

Apoptosis was quantified using an Annexin V-FITC Apoptosis Detection Kit (Beyotime, Nantong, China). Briefly, ARPE-19 cells were seeded in 6-well plates at a density of 4×10^6 cells/ml. After the cells were treated, they were harvested by trypsinization. Then, the cells were centrifuged and washed twice with cold PBS. Between 1×10^5 and 1×10^6 cells were resuspended in 300 µl of 1× binding buffer and then transferred to a sterile glass flow cytometry tube. In total, 5 µl of annexin V-FITC was added to the suspension, and then the suspension was incubated in the dark for 30 min at room temperature. Next, the cells were incubated in the dark with 5 µl of PI and analyzed using a flow cytometer (FACS Partec, Germany).

Measurement of mitochondrial membrane potential (ΔΨm)

ΔΨm was analyzed by JC-1 assay (Beyotime, Nantong, China). JC-1 is a cationic dye that indicates ΔΨm by reversibly shifting its fluorescence emission between green and red. Briefly, a staining mixture of 300 nM JC-1 was prepared according to the manufacturer's instructions. Cells were incubated with the staining mixture for 30 min at 37°C. Next, the cells were washed twice with medium and finally resuspended in fresh medium. ΔΨm was monitored using a fluorescence microscope.

Plasmid construction

The PRDX6-pcDNA3.1 vector was generated from the human PRDX6 sequence obtained from GenBank (PRDX6; GenBank accession no. NM_004905.2). PRDX6 was cut with the restriction enzymes EcoRI and XhoI, and then PRDX6 was inserted into a pcDNA3.1 vector (Invitrogen, USA) for sequencing. STK33 siRNA oligos were inserted into the pSilencer 4.1-CMV plasmid using BamHI and HindIII enzyme sites. All transfection experiments were repeated in independent triplicates.

Cell transfection

Cells were transfected with the indicated PRDX6 plasmids or siRNAs using Lipofectamine 2000 (Invitrogen, USA) in serum-free medium according to the manufacturer's instructions. The cells were collected after 24 h of transient transfection for further experiments.

Real-time qPCR

Total RNA from ARPE-19 cells was isolated using TRIzol Reagent (TaKaRa, Japan) according to the manufacturer's protocol. The RNA concentration was quantitated by measuring the absorbance at 260 nm, and the RNA purity was determined by the A260/A280 ratio. The total RNA (1 μg) from each tissue sample was reverse-transcribed to cDNA using a Prime Script RT Reagent Kit (TaKaRa) in the following reaction system: 8 μl of 5× Prime Script Buffer (for real-time), 2 μl of Prime Script RT Enzyme Mix, 0.1 nmol oligo(dT) primer, 0.2 nM random hexamers, 2 μg of total RNA, and RNase-free deionized water to a final volume of 40 μl. The reverse transcription program was as follows: 15 min at 37°C and 5 sec at 85°C. The specific primers were designed using Primer Premier 5.0. All primers were synthesized by Sangon Biotechnology. An ABI 7300 Real-Time PCR System (ABI, USA) was used for RT-PCR amplification and detection. RT-PCR reactions were prepared in triplicates in 20-μl reaction volumes as follows: 10 μl of 2× SYBR Premix Ex Taq II, 0.4 μM forward and reverse primers, 2 μl of cDNA (50 ng) template, and 6.4 μl of RNase-free water. Master Mix without cDNA template was used as a negative control. RT-PCR cycling conditions were used as suggested in the SYBR Premix Ex Taq II Kit (TaKaRa, Japan) instructions. Melting curves were checked to ensure the specificity of the PCR products in the SYBR Green reactions. Relative mRNA levels of the target genes were normalized to β-actin mRNA. The PRDX6 primer sequences used were F: GGAGCAAGGATATCAATGCTTACA and R: CCAAAAACAAACACCACACGA.

Western blot analysis

Cells were washed twice in ice-cold PBS and resuspended in protein lysis buffer (Beyotime, China) containing a protease inhibitor cocktail. The supernatants were centrifuged at 10,000 × *g* for 15 min at 4°C to obtain the protein supernatants. Protein concentrations were determined using Bio-Rad protein assay kits (Bio-Rad, USA). Then, the samples were separated by SDS-PAGE on 10% polyacrylamide gels and electro-transferred to Hybond polyvinylidene fluoride (PVDF) membranes. The PVDF membranes were soaked for 2 h at room temperature with 5% nonfat milk in TBST buffer composed of 50 mM Tris (pH 7.6), 150 mM NaCl and 0.1% Tween-20 and then incubated with primary antibody overnight at 4°C. After the membranes were washed three times with TBST buffer for 5 min each, they were incubated at room temperature for 2 h in TBST containing horseradish peroxidase (HRP)-conjugated goat anti-mouse or goat anti-rabbit IgG antibody (Santa Cruz, Inc., USA). Next, the membranes were washed three times with TBST buffer for 10 min each. Then, the membranes were incubated in ECL reagent (Pierce, Thermo Co., Ltd, USA) for HRP detection and exposed to autoradiography film (Bio-Rad, Co., Ltd, USA) for band visualization. β-Actin was used as a loading control. The relative amounts of various proteins were analyzed, and the results were quantified using ImageJ software.

Fluorescence microscopy and indirect immunofluorescence staining

Cells were grown in 6-well glass-bottomed dishes. After the cells were treated, they were fixed in 4% paraformaldehyde for 30 min and then permeabilized with 0.2% Triton X-100 in PBS. Nonspecific binding sites were blocked with normal goat serum (Sigma-Aldrich, USA) diluted in 0.1% Triton-X-100 in PBS for 2 h. Then, the cells were incubated overnight at 4°C with primary antibodies at a 1:200 dilution in blocking buffer. Anti-p-AKT antibody was purchased from Proteintech Technology Company. The next day, the cells were incubated with appropriate fluorophore-conjugated secondary antibodies. DAPI was used to stain nuclei before acquiring images. The images were acquired using a fluorescence microscope.

Results

H_2O_2 and blue light can induce cell death and oxidative stress in ARPE-19 cells

The redox reaction is a basic biochemical reaction in human bodies that is indispensable for cellular survival. However, when the cells in our bodies suffer from harmful factors that disrupt this balance, they can be injured and eventually undergo apoptosis [18, 19]. In this study, we exposed ARPE-19 cells to H_2O_2 together with blue light to generate an oxidative stress injury model. ARPE-19 is a human RPE cell line with an epithelial morphology and a rapid proliferation rate. To confirm that H_2O_2 together with blue light (subsequently referred to simply as "H_2O_2") could affect cell survival and oxidative stress, we first treated ARPE-19

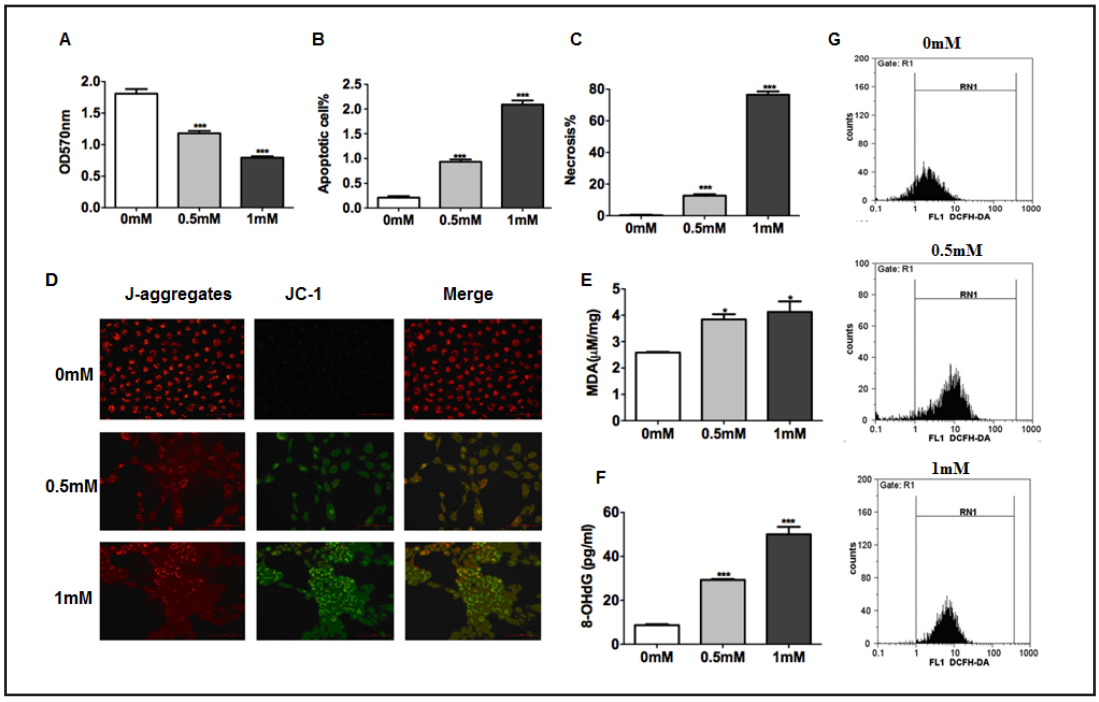

Fig. 1. H_2O_2 and blue light induced oxidative stress and cell death in ARPE-19 cells. ARPE-19 cells were treated with various doses of H_2O_2 (0, 0.5, 1.0 mM) for 24 h under blue light. (A) Cell viability was analyzed by MTT assay. (B and C) After annexin V/PI double staining, apoptosis (B) and necrosis (C) were quantified by flow cytometry. (D) H_2O_2-treated ARPE-19 cells showed a reduction in ΔΨm. (E) MDA concentrations of cells were detected by MDA assay. (F) 8-OHdG concentrations in cells were determined by 8-OHdG assay. (G) Cells were stained with DCF-DA to detect intracellular ROS production. The values represent the mean ± S.D. of three independent experiments. Statistical significance was assessed with one-way ANOVA plus Tukey's test using GraphPad Prism software (*p < 0.05; **p < 0.01; ***p < 0.001 *vs.* control).

cells with different concentrations of H_2O_2 (0, 0.5 and 1.0 mM) under blue light for 24 h and then detected cell proliferation by MTT assay. We found that H_2O_2 could inhibit cell growth in a dose-dependent manner, with 50% of cell growth inhibited at 1 mM H_2O_2 (Fig. 1A). These results indicated that H_2O_2 and blue light might induce apoptosis in ARPE-19 cells. Next, using annexin V/PI double staining, we detected the apoptotic effect of H_2O_2 on ARPE-19 cells. Using flow cytometry, we found that H_2O_2 significantly increased both the apoptotic (Fig. 1B) and necrotic (Fig. 1C) populations of ARPE-19 cells at 24 h. These findings indicated that H_2O_2 induced apoptosis and necrosis in ARPE-19 cells. In addition, we examined the effect of H_2O_2 on the ΔΨm. We observed that H_2O_2-treated cells exhibited significantly more green JC-1 fluorescence compared to control cells under a fluorescence microscope, which suggested a reduction in the ΔΨm in H_2O_2-treated ARPE-19 cells (Fig. 1D).

In subsequent experiments using MDA and 8-OHdG assays, we found that the oxidative stress end products MDA and 8-OHdG increased in a dose-dependent manner in H_2O_2-treated cells compared to control cells (Fig. 1E, F). To further determine the effect of H_2O_2 on ROS induction, we measured intracellular ROS production using DCF-DA fluorescence dye. As expected, we found that H_2O_2 significantly enhanced intracellular ROS production in a dose-dependent manner (Fig. 1G). Taken together, these data suggested that H_2O_2 could induce oxidative damage in ARPE-19 cells.

PRDX6 mRNA levels increase after H2O2 and blue light stimulation in ARPE-19 cells

PRDX6 serves as an antioxidant and plays an important role in the maintenance of redox balance. To detect whether PRDX6 was involved in H_2O_2-induced cellular injury, we first quantified PRDX6 mRNA expression by real-time PCR. As shown in Fig. 2A, we observed

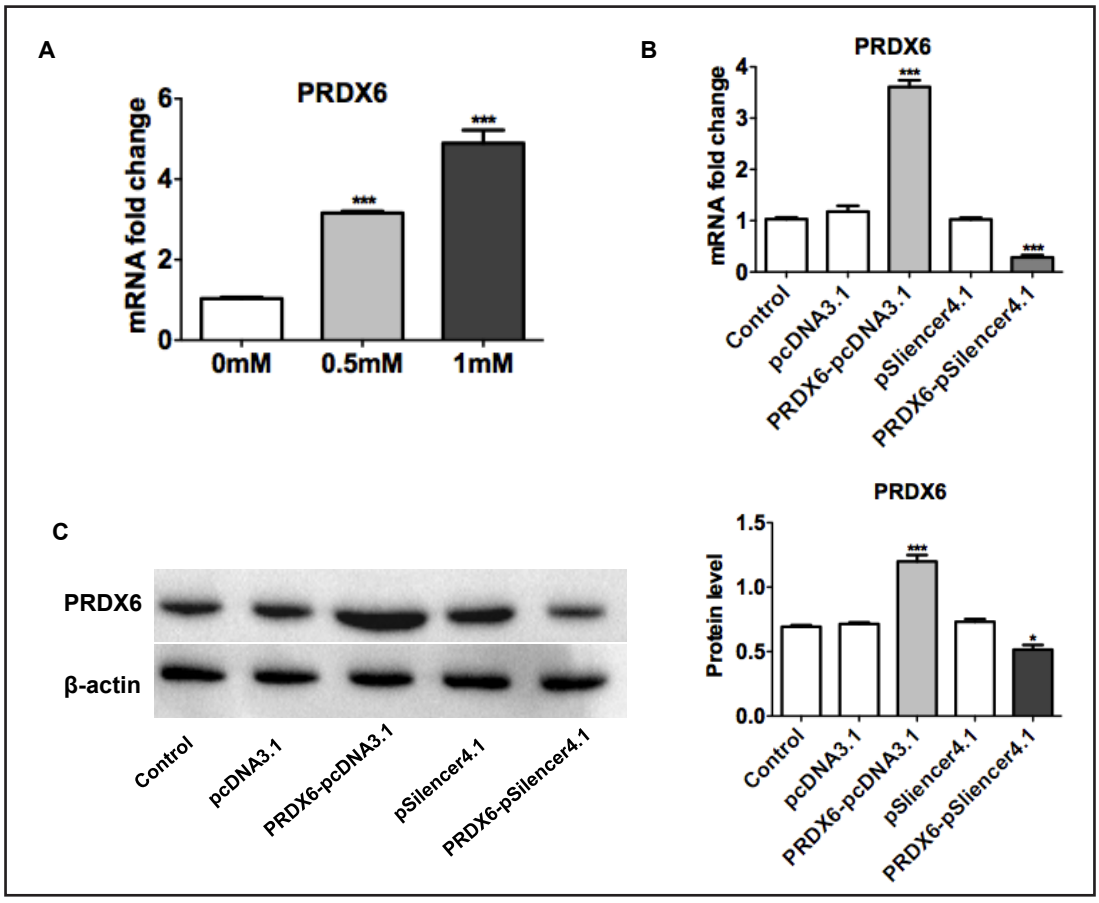

Fig. 2. PRDX6 expression significantly increased after stimulation with H_2O_2 and blue light. ARPE-19 cells were treated with H_2O_2 for 24 h under blue light. (A) Relative gene expression of PRDX6 was detected by real-time PCR in ARPE-19 cells with and without varying doses of H_2O_2 stimulation and blue light. Stimulations were performed using 0, 0.5 and 1.0 mM H_2O_2 for 24 h (n = 3). The results are presented as the average fold change in PRDX6 gene expression (normalized to β-actin) after 24 h of 0, 0.5, and 1.0 mM H_2O_2 and blue light exposure. (B) qPCR analysis was performed using isolated total RNA to quantify PRDX6 mRNA levels after PRDX6-pcDNA3.1 and PRDX6 siRNA transfection. (C) The expression of PRDX6 protein was detected by western blot after PRDX6-pcDNA3.1 and PRDX6 siRNA transfection. The data are representative of three experiments with similar results (Student's t-test, $*p < 0.05$). β-Actin was used as the loading control.

that PRDX6 mRNA expression significantly increased after H_2O_2 treatment (24 h) in a dose-dependent manner (approximately 5-fold increase at 1 mM H_2O_2). To investigate the role of PRDX6 further, we generated a PRDX6 overexpressing plasmid (PRDX6-pcDNA3.1) and a silencing plasmid (PRDX6-pSilencer 4.1). The transfection efficiencies of PRDX6-pcDNA3.1 and PRDX6-pSilencer 4.1 were confirmed by both qPCR and western blot assays (Fig. 2B, C). Both plasmids achieved the highest transfection efficiencies (more than 50%) at 48 h post-transfection (Fig. 2B, C).

PRDX6 can protect ARPE-19 cells from cell death and oxidative stress induced by H2O2 and blue light

To determine whether PRDX6 played a role in H_2O_2-induced cell death and oxidative injury in ARPE-19 cells, we first transfected these cells with PRDX6-pcDNA3.1 or PRDX6-pSilencer 4.1 and then exposed them to H_2O_2 (0.5 or 1.0 mM) and blue light treatment for 24 h. Flow cytometric assay indicated that PRDX6 overexpression decreased the population of apoptotic (Fig. 3A) or necrotic (Fig. 3B) cells. In addition, using JC-1 immunostaining, PRDX6 overexpression increased the $\Delta\Psi m$ induced by H_2O_2 (Fig. 3C). In contrast, PRDX6 knockdown

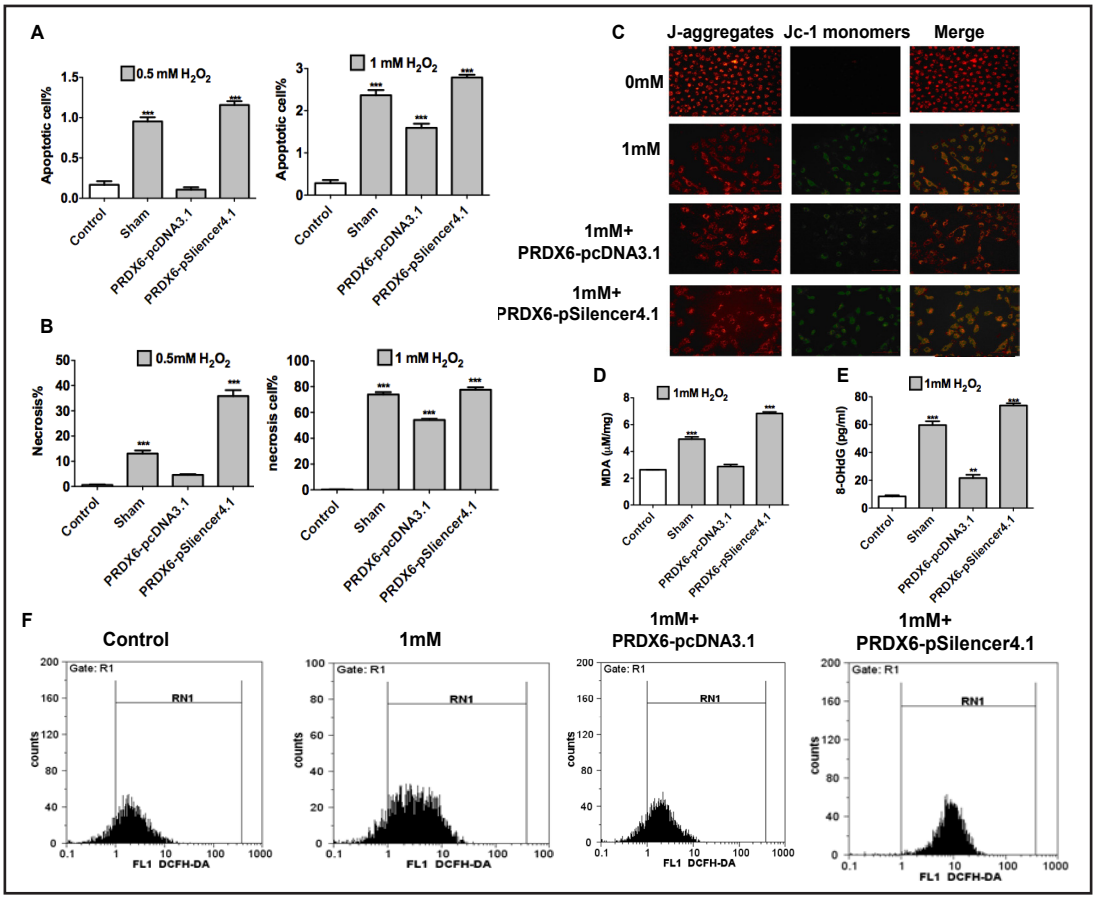

Fig. 3. PRDX6 protected ARPE-19 cells from undergoing oxidative stress and cell death induced by H_2O_2 and blue light. ARPE-19 cells were transfected with the PRDX6-pSilencer 4.1 plasmid or the PRDX6-pcDNA3.1 overexpression plasmid, and the cells were allowed to recover in regular culture medium. At 24 h post-transfection, the cells were exposed to 0.5 or 1.0 mM H_2O_2 and blue light for 24 h. (A, B) Apoptosis (A) and necrosis (B) were determined by annexin V/PI double staining, followed by flow cytometry. (C) Cells were treated as above. After immunostaining, the green fluorescence of JC-1 monomer and red fluorescence of J-aggregates were clustered in groups. (D) MDA concentration in cells was detected by MDA assay. (E) 8-OHdG concentration in cells was tested by 8-OHdG assay. (F) The cells were stained with DCF-DA to detect intracellular ROS production. The values represent the mean ± S.D. of three independent experiments. Statistical significance was assessed using one-way ANOVA plus Tukey's test using GraphPad Prism Version 5.0a software (*$p < 0.05$; **$p < 0.01$; ***$p < 0.001$ *vs.* control).

increased the population of dead cells and decreased H_2O_2-induced changes to the ΔΨm (Fig. 3A-C). Moreover, we found that MDA and 8-OHdG decreased following PRDX6 overexpression (Fig. 3D, E). Similarly, intracellular ROS production was further confirmed by flow cytometry, followed by probing with DCF-DA at 488 nm excitation. Compared to the H_2O_2-treated group, we found that knocking down PRDX6 with PRDX6-pSilencer 4.1 significantly increased intracellular ROS production, while overexpressing PRDX6 with PRDX6-pcDNA3.1 decreased ROS production (Fig. 3F). Together, these observations demonstrated that PRDX6 might be a protective gene in the H_2O_2 induced-ARPE-19 cell injury model.

PRDX6 protection against H2O2-induced cellular injury partially functions through PI3K/AKT signaling

PI3K/AKT signaling plays an important role in cell growth and cellular oxidative stress [20]. Therefore, in this study we investigated the role of PI3K/AKT signaling in PRDX6

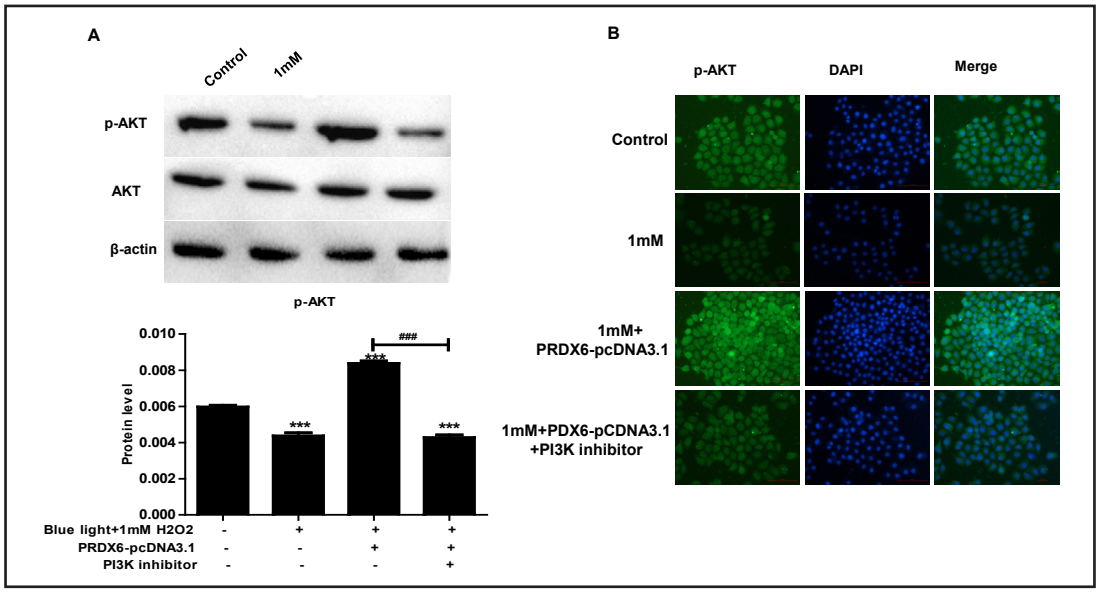

Fig. 4. PI3K/AKT signaling is regulated by PRDX6. Cells transfected with different PRDX6 plasmids were incubated with or without 10 μM LY294002 for 1 h and then exposed to 1 mM H_2O_2 and blue light for 24 h. (A) Cells were treated as described above, and p-AKT expression was detected by western blot analysis. (B) p-AKT expression was observed under a fluorescence microscope after immunostaining. DAPI was used to stain the nuclei. The values represent the mean ± S.D. of three independent experiments. Statistical significance was assessed using one-way ANOVA plus Tukey's test using GraphPad Prism Version 5.0a software (*p < 0.05; **p < 0.01; ***p < 0.001 *vs.* control; $^{\#}$p < 0.05; $^{\#\#}$p < 0.01; $^{\#\#\#}$p < 0.001, *vs.* 1 mM H_2O_2 + blue light + PRDX6-pcDNA3.1 group).

protection against oxidative damage. After H_2O_2 treatment, we found that the p-AKT level significantly decreased, suggesting the involvement of p-AKT (Fig. 4A) in this oxidative injury cellular model. Western blot analysis indicated that the decreased p-AKT level induced by H_2O_2 recovered significantly upon PRDX6 overexpression (Fig. 4A). The level of p-AKT was further confirmed by fluorescence microscopy (Fig. 4B). To confirm the effect of p-AKT, we incubated cells with 10 μM LY294002 for 1 h before H_2O_2 treatment. This synthetic inhibitor of the PI3K/AKT signaling pathway [21] clearly inhibited increased AKT phosphorylation by PRDX6 overexpression (Fig. 4A, B). To assess the extent to which cell growth and ROS production occurred downstream of the PI3K/AKT signaling pathway, we co-treated cells with PRDX6-pcDNA and LY294002 and tested their effects on cell growth and ROS production. We found that the alleviation of cell apoptosis and necrosis induced by PRDX6 overexpression significantly increased upon PI3K/AKT inhibitor treatment (Fig. 5A, B). Similar results were observed by JC-1 assay (Fig. 5C). Moreover, we found that the alleviation of ROS production by PRDX6 overexpression significantly increased upon PI3K/AKT inhibition (Fig. 5D). Together, these results indicated that PRDX6 protected against H_2O_2-induced cell injury through the PI3K/AKT pathway.

Discussion

Previous ophthalmological studies have focused extensively on the crucial role of oxidative stress in the pathophysiology of age-related macular degeneration (AMD) [22]. Recently, some investigators hypothesized that oxidative stress could be linked to the occurrence of HRD [23]. In the present study, we used ARPE-19 cells challenged with oxidative stress (H_2O_2 and blue light) as an *in vitro* HRD model to study the underlying mechanism of oxidative damage in HRD. Considering the physiological function and location of RPE

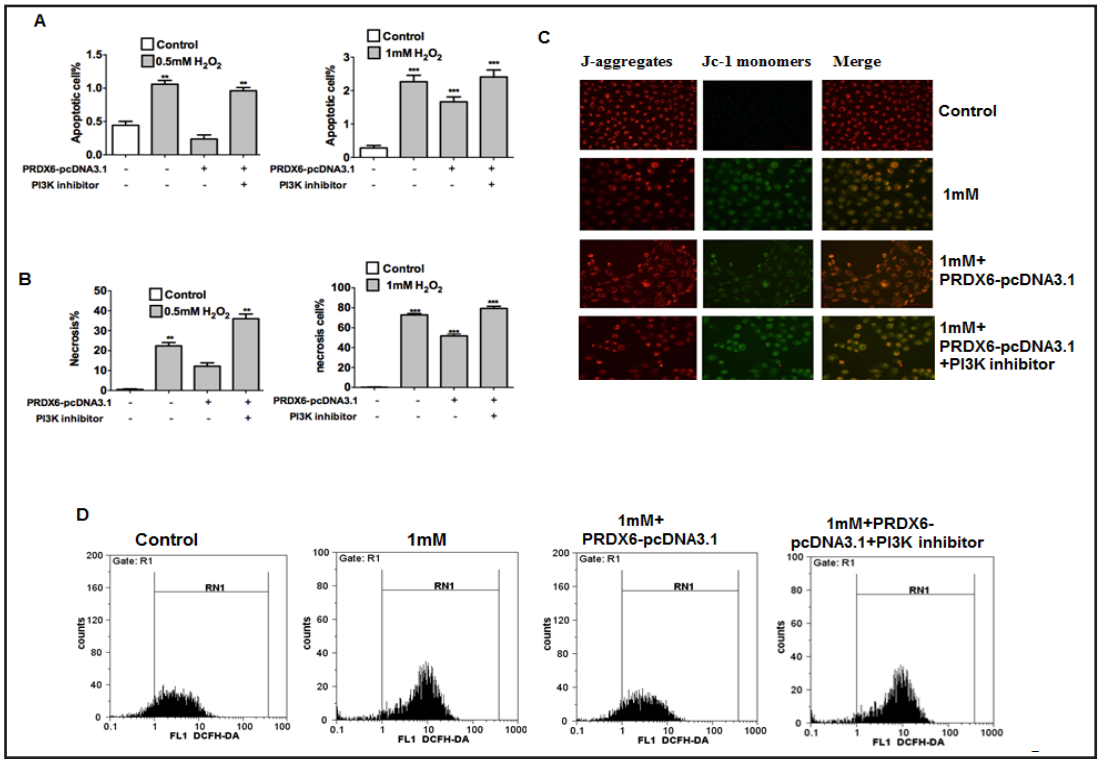

Fig. 5. The PRDX6 gene activated the PI3K/AKT signaling pathway to protect ARPE-19 cells against oxidative stress and cell death. Cells transfected with different PRDX6 plasmids were incubated with or without 10 μM LY294002 for 1 h and then exposed to 0.5 or 1 mM H_2O_2 and blue light for 24 h. (A and B) Apoptosis (A) and necrosis (B) were determined by flow cytometry after annexin V/PI double staining. (C) After treatment, the cells were immunostained using a JC-1 kit. The green fluorescence of JC-1 monomers and red fluorescence of J-aggregates clustered in groups. (D) Cells were stained with DCF-DA to detect intracellular ROS production. The values represent the mean ± S.D. of three independent experiments. Statistical significance was assessed using one-way ANOVA plus Tukey's test using GraphPad Prism Version 5.0a software (*$p < 0.05$; **$p < 0.01$; ***$p < 0.001$ *vs.* control; $^{\#}p < 0.05$; $^{\#\#}p < 0.01$; $^{\#\#\#}p < 0.001$, *vs.* 1 mM H_2O_2 + blue light + PRDX6-pcDNA3.1 group).

cells, which lead them to be constantly exposed to many ROS [24, 25], the protection of RPE cells from oxidative stress and damage might serve as an excellent target for treating HRD. Therefore, RPE cells seemed to be an ideal model for HRD study. Here, we used the human RPE cell line ARPE-19 and. We used H_2O_2 and blue light to induce oxidative stress in these cells. H_2O_2-induced oxidative stress is a classic model by which researchers have detected susceptibility to oxidative stress or antioxidant efficiency in RPE cells [26-28]. Additionally, light exposure has been linked to the occurrence and development of AMD possibly through oxidative stress-related pathology [29, 30]. While blue light illumination induced a variety of ROS in RPE cells and increased ROS production by mitochondria, light-induced oxidation has also been positively associated with age [31, 32]. We used the fluorescent dye DCF-DA to quantify ROS generation, which is not a direct assay of H_2O_2, NO, lipid peroxides, singlet O_2 or O_2^- production. We observed that H_2O_2 and blue light irradiation together could induce robust oxidative stress (Fig. 1E-G). However, additional studies to specify the pool of hydrogen peroxide are warranted. Furthermore, apoptosis and necrosis significantly increased in the H_2O_2-treated group. These results demonstrated that H_2O_2 could induce oxidative stress in ARPE-19 cells and suggested that this treatment could be used to stimulate the disease model in our study. In this paper, we used both H_2O_2 and blue light to increase oxidative stress and to decrease antioxidant efficiency in ARPE-19 cells.

When we explored the mechanism of H_2O_2-induced cellular oxidative stress, we hypothesized that PRDX6 could be involved. The mRNA expression levels of PRDX6 significantly increased after H_2O_2 treatment (Fig. 2A). Similar results were also found in other oxidative stress models. The mRNA and protein expression and enzymatic activity of PRDX6 markedly increase in the mouse when exposed to 100% oxygen [33]. Additionally, two-dimensional electrophoresis and mass spectrometry analyses of retinas of mice with HRD indicated higher PRDX6 expression [34]. In the present study, we demonstrated for the first time that PRDX6 could protect ARPE-19 cells against oxidative damage by H_2O_2. PRDX6 played an important role in resisting oxidative stress and in maintaining the balance of phospholipid metabolism. In addition, transiently overexpressing PRDX6 significantly decreased cell viability and increased apoptosis induced by H_2O_2 and blue light (Fig. 3A, B). These findings were consistent with previous observations in other disease models, where PRDX6 protein exerted essential protective effects against organ damage induced by a variety of stressors such as ischemia-reperfusion, oxidative stress, and lipopolysaccharide [35-37]. In one study, PRDX6 transgenic mice displayed significantly decreased oxidative damage induced by tobacco [38].

To explore factors downstream of PRDX6 in HRD, we assessed potential cell signaling pathways in cells after H_2O_2 treatment. We observed that p-AKT signaling, which is an important signaling pathway in ARPE-19 cells [39], significantly decreased in ARPE-19 cells when treated with H_2O_2 and blue light (24 h). PI3K/AKT signaling is a critical pathway that is involved in cell growth, survival, apoptosis, and other cellular functions [40]. However, previous studies have shown that AKT can be activated in RPE cells as early as 15 min after H_2O_2 stimulation [41]. This finding may be explained by several factors, including the differences in injury models (H_2O_2 *vs.* H_2O_2 and blue light), different treatment periods (15 min *vs.* 24 h), and different cells (primary cells *vs.* cell lines). Here, we further confirmed the role of AKT by introducing LY294002, a highly specific inhibitor of PI3K/AKT signaling. Upon LY294002 treatment, ROS production and apoptosis significantly increased in ARPE-19 cells under oxidative stress conditions (Fig. 5). In addition, after PRDX6 overexpression, H_2O_2-induced decreases in p-AKT levels were significantly ameliorated (Fig. 4A). These results indicated that AKT is a downstream factor of PRDX6 that drives redox balance during stress. However, we cannot exclude other factors also contributing to this signaling pathway, thus warranting further investigation of the underlying mechanism of this effect.

Taken together, our results showed that H_2O_2 and blue light could significantly induce oxidative stress and cell apoptosis in ARPE-19 cells. We further found that PRDX6 could protect ARPE-19 cells against oxidative damage induced by H_2O_2 and blue light. In addition, we revealed a link between PRDX6 and AKT in directly contributing to oxidative stress and cell survival after H_2O_2 stimulation. Collectively, these observations provided new insight into the role of PRDX6 in resisting oxidative stress and could indicate novel targets for clinical intervention.

Acknowledgments

The authors thank the College of the Second Affiliated Hospital of Kunming Medical University for their excellent assistance and use of their many instruments. This study was funded by the Applied Basic Research Program of Yunnan Province (grant no. 2012FB058).

Disclosure Statement

The authors declare that no financial or commercial conflicts of interest exist.

References

1 Goodwin P: Hereditary retinal disease. Curr Opin Ophthalmol 2008;19:255-262.
2 Wright AF, Chakarova CF, Abd El-Aziz MM, Bhattacharya SS: Photoreceptor degeneration: Genetic and mechanistic dissection of a complex trait. Nat Rev Genet 2010;11:273-284.
3 Al-Merjan JI, Pandova MG, Al-Ghanim M, Al-Wayel A, Al-Mutairi S: Registered blindness and low vision in kuwait. Ophthalmic Epidemiol 2005;12:251-257.
4 Kuznetsova AV, Kurinov AM, Aleksandrova MA: Cell models to study regulation of cell transformation in pathologies of retinal pigment epithelium. J Ophthalmol 2014;2014:801787.
5 Shen J, Yang X, Dong A, Petters RM, Peng YW, Wong F, Campochiaro PA: Oxidative damage is a potential cause of cone cell death in retinitis pigmentosa. J Cell Physiol 2005;203:457-464.
6 Punzo C, Kornacker K, Cepko CL: Stimulation of the insulin/mtor pathway delays cone death in a mouse model of retinitis pigmentosa. Nat Neurosci 2009;12:44-52.
7 Vlachantoni D, Bramall AN, Murphy MP, Taylor RW, Shu X, Tulloch B, Van Veen T, Turnbull DM, McInnes RR, Wright AF: Evidence of severe mitochondrial oxidative stress and a protective effect of low oxygen in mouse models of inherited photoreceptor degeneration. Hum Mol Genet 2011;20:322-335.
8 Ho N, Brookshire BR, Clark JE, Lucki I: Indomethacin reverses decreased hippocampal cell proliferation in streptozotocin-induced diabetic mice. Metab Brain Dis 2014
9 Dillioglugil MO, Kir HM, Demir C, Ilbay G, Sahin D, Dillioglugil O, Bambal G, Mekik H, Ates N: Effect of pentylenetetrazole and sound stimulation induced single and repeated convulsive seizures on the mda, gsh and no levels, and sod activities in rat liver and kidney tissues. Brain Res Bull 2010;83:356-359.
10 Kanth BK, Jnawali HN, Niraula NP, Sohng JK: Superoxide dismutase (sod) genes in streptomyces peucetius: Effects of sods on secondary metabolites production. Microbiol Res 2011;166:391-402.
11 Yen CC, Lai YW, Chen HL, Lai CW, Lin CY, Chen W, Kuan YP, Hsu WH, Chen CM: Aerosolized human extracellular superoxide dismutase prevents hyperoxia-induced lung injury. PLoS One 2011;6:e26870.
12 Oshikawa J, Urao N, Kim HW, Kaplan N, Razvi M, McKinney R, Poole LB, Fukai T, Ushio-Fukai M: Extracellular sod-derived h2o2 promotes vegf signaling in caveolae/lipid rafts and post-ischemic angiogenesis in mice. PLoS One 2010;5:e10189.
13 Shichi H, Demar JC: Non-selenium glutathione peroxidase without glutathione s-transferase activity from bovine ciliary body. Exp Eye Res 1990;50:513-520.
14 Kim SY, Jo HY, Kim MH, Cha YY, Choi SW, Shim JH, Kim TJ, Lee KY: H2o2-dependent hyperoxidation of peroxiredoxin 6 (prdx6) plays a role in cellular toxicity via up-regulation of ipla2 activity. J Biol Chem 2008;283:33563-33568.
15 Manevich Y, Sweitzer T, Pak JH, Feinstein SI, Muzykantov V, Fisher AB: 1-cys peroxiredoxin overexpression protects cells against phospholipid peroxidation-mediated membrane damage. Proc Natl Acad Sci U S A 2002;99:11599-11604.
16 Kumin A, Schafer M, Epp N, Bugnon P, Born-Berclaz C, Oxenius A, Klippel A, Bloch W, Werner S: Peroxiredoxin 6 is required for blood vessel integrity in wounded skin. J Cell Biol 2007;179:747-760.
17 Pak JH, Manevich Y, Kim HS, Feinstein SI, Fisher AB: An antisense oligonucleotide to 1-cys peroxiredoxin causes lipid peroxidation and apoptosis in lung epithelial cells. J Biol Chem 2002;277:49927-49934.
18 Xu ZS, Wang XY, Xiao DM, Hu LF, Lu M, Wu ZY, Bian JS: Hydrogen sulfide protects mc3t3-e1 osteoblastic cells against h2o2-induced oxidative damage-implications for the treatment of osteoporosis. Free Radic Biol Med 2011;50:1314-1323.
19 Moon DO, Kim BY, Jang JH, Kim MO, Jayasooriya RG, Kang CH, Choi YH, Moon SK, Kim WJ, Ahn JS, Kim GY: K-ras transformation in prostate epithelial cell overcomes h2o2-induced apoptosis via upregulation of gamma-glutamyltransferase-2. Toxicol In Vitro 2012;26:429-434.
20 Nakanishi A, Wada Y, Kitagishi Y, Matsuda S: Link between pi3k/akt/pten pathway and nox proteinin diseases. Aging Dis 2014;5:203-211.
21 Choi EM: Luteolin protects osteoblastic mc3t3-e1 cells from antimycin a-induced cytotoxicity through the improved mitochondrial function and activation of pi3k/akt/creb. Toxicol In Vitro 2011;25:1671-1679.
22 Beatty S, Koh H, Phil M, Henson D, Boulton M: The role of oxidative stress in the pathogenesis of age-related macular degeneration. Surv Ophthalmol 2000;45:115-134.
23 Hanus J, Zhang H, Wang Z, Liu Q, Zhou Q, Wang S: Induction of necrotic cell death by oxidative stress in retinal pigment epithelial cells. Cell Death Dis 2013;4:e965.

24 Cai J, Nelson KC, Wu M, Sternberg P, Jr., Jones DP: Oxidative damage and protection of the rpe. Prog Retin Eye Res 2000;19:205-221.
25 Liang FQ, Godley BF: Oxidative stress-induced mitochondrial DNA damage in human retinal pigment epithelial cells: A possible mechanism for rpe aging and age-related macular degeneration. Exp Eye Res 2003;76:397-403.
26 Kaczara P, Sarna T, Burke JM: Dynamics of h2o2 availability to arpe-19 cultures in models of oxidative stress. Free Radic Biol Med 2010;48:1064-1070.
27 Geiger RC, Waters CM, Kamp DW, Glucksberg MR: Kgf prevents oxygen-mediated damage in arpe-19 cells. Invest Ophthalmol Vis Sci 2005;46:3435-3442.
28 Zareba M, Raciti MW, Henry MM, Sarna T, Burke JM: Oxidative stress in arpe-19 cultures: Do melanosomes confer cytoprotection? Free Radic Biol Med 2006;40:87-100.
29 Taylor HR, West S, Munoz B, Rosenthal FS, Bressler SB, Bressler NM: The long-term effects of visible light on the eye. Arch Ophthalmol 1992;110:99-104.
30 Cano M, Thimmalappula R, Fujihara M, Nagai N, Sporn M, Wang AL, Neufeld AH, Biswal S, Handa JT: Cigarette smoking, oxidative stress, the anti-oxidant response through nrf2 signaling, and age-related macular degeneration. Vision Res 2010;50:652-664.
31 Rozanowska M, Jarvis-Evans J, Korytowski W, Boulton ME, Burke JM, Sarna T: Blue light-induced reactivity of retinal age pigment. In vitro generation of oxygen-reactive species. J Biol Chem 1995;270:18825-18830.
32 King A, Gottlieb E, Brooks DG, Murphy MP, Dunaief JL: Mitochondria-derived reactive oxygen species mediate blue light-induced death of retinal pigment epithelial cells. Photochem Photobiol 2004;79:470-475.
33 Kim HS, Manevich Y, Feinstein SI, Pak JH, Ho YS, Fisher AB: Induction of 1-cys peroxiredoxin expression by oxidative stress in lung epithelial cells. Am J Physiol Lung Cell Mol Physiol 2003;285:L363-369.
34 Zheng Q, Ren Y, Tzekov R, Zhang Y, Chen B, Hou J, Zhao C, Zhu J, Zhang Y, Dai X, Ma S, Li J, Pang J, Qu J, Li W: Differential proteomics and functional research following gene therapy in a mouse model of leber congenital amaurosis. PLoS One 2012;7:e44855.
35 Godoy JR, Oesteritz S, Hanschmann EM, Ockenga W, Ackermann W, Lillig CH: Segment-specific overexpression of redoxins after renal ischemia and reperfusion: Protective roles of glutaredoxin 2, peroxiredoxin 3, and peroxiredoxin 6. Free Radic Biol Med 2011;51:552-561.
36 Yang D, Song Y, Wang X, Sun J, Ben Y, An X, Tong L, Bi J, Wang X, Bai C: Deletion of peroxiredoxin 6 potentiates lipopolysaccharide-induced acute lung injury in mice. Crit Care Med 2011;39:756-764.
37 Tulsawani R, Kelly LS, Fatma N, Chhunchha B, Kubo E, Kumar A, Singh DP: Neuroprotective effect of peroxiredoxin 6 against hypoxia-induced retinal ganglion cell damage. BMC Neurosci 2010;11:125.
38 Lee KO, Jang HH, Jung BG, Chi YH, Lee JY, Choi YO, Lee JR, Lim CO, Cho MJ, Lee SY: Rice 1cys-peroxiredoxin over-expressed in transgenic tobacco does not maintain dormancy but enhances antioxidant activity. FEBS Lett 2000;486:103-106.
39 Klettner A: Oxidative stress induced cellular signaling in rpe cells. Front Biosci (Schol Ed) 2012;4:392-411.
40 Krasilnikov MA: Phosphatidylinositol-3 kinase dependent pathways: The role in control of cell growth, survival, and malignant transformation. Biochemistry (Mosc) 2000;65:59-67.
41 Yang P, Peairs JJ, Tano R, Jaffe GJ: Oxidant-mediated akt activation in human rpe cells. Invest Ophthalmol Vis Sci 2006;47:4598-4606.